

HOW TO BUILD STABLE GEOCHEMICAL RESERVOIRS ON MARS? A. C. Plesa¹, N. Tosi¹ and D. Breuer¹ (DLR, Institute of Planetary Research, Rutherfordstr. 2, 12489 Berlin, ana.plesa@dlr.de).

Introduction: Little attention has been devoted so far to find a modeling framework able to explain the geophysical implications of the data obtained from the analysis of the Martian meteorites (Shergottites, Nakhilites, Chassignites). Geochemical investigations of these samples imply the presence of at least three isotopically distinct reservoirs that formed early in the planet's history and remained separate over the entire thermo-chemical evolution of Mars. Two of these reservoirs are depleted in incompatible lithophile elements relative to chondrites and are most likely located in the Martian mantle, while the third one is enriched and may reside either in the crust or in the mantle [1, 2].

Model and Methods: In this work we study the formation and stability of geochemical reservoirs in the Martian mantle. To this end, we use either the 2D Cartesian box code YACC [3] or the 2D cylindrical – 3D spherical global mantle convection code Gaia [4], to investigate under which circumstances mantle reservoirs can form and remain stable over the entire planetary evolution.

We consider different scenarios for the formation of mantle reservoirs. First we investigate the consequences of reservoir formation through fractional crystallization of a global magma ocean, which results in an unstably stratified mantle density profile. The subsequent overturn of such unstable configuration has been suggested to create a stably stratified mantle with large density gradients capable to keep the mantle heterogeneous and to prevent mixing due to thermal convection [5, 6].

Using systems heated either solely from below or from within, constant or temperature-dependent viscosity and a simplified linear unstable density profile as initial condition, we derive scaling laws that relate the time over which chemical heterogeneities can be preserved (mixing time) to the buoyancy ratio B , which measures the relative importance of chemical to thermal buoyancy. Additionally, we run thermal evolution models with cooling boundary conditions and decay of radioactive elements, where a detailed magma ocean crystallization sequence as obtained from geochemical modeling [5] is employed. We account for a chemical phase transition between lower and upper mantle, and assume all radiogenic heat sources to be enriched during the freezing-phase of the magma ocean in the uppermost 50 km [7].

In a second scenario, we consider partial melting effects like mantle depletion in crustal components and its associated density variations as main mechanism for

the formation of mantle reservoirs. Additionally, we account for dehydration stiffening due to water extraction and outgassing during the melting process, and formation of an insulating crust enriched in heat producing elements.

Results: In the first scenario, the overturn of a fractionally crystallized global magma ocean may lead to a stable density configuration depending on the density gradient used and hence the buoyancy ratio. We find that the mixing time increases exponentially with B (Fig. 1a). With a temperature-dependent viscosity (blue line in Fig. 1a), for buoyancy ratios larger than ~ 0.5 (corresponding to a chemical density contrast of $\sim 60 \text{ kg/m}^3$), chemical heterogeneities can be preserved over the entire planet's history. The higher is B , the higher is the tendency of the chemical stratification to suppress any form of thermal convection and mixing [8].

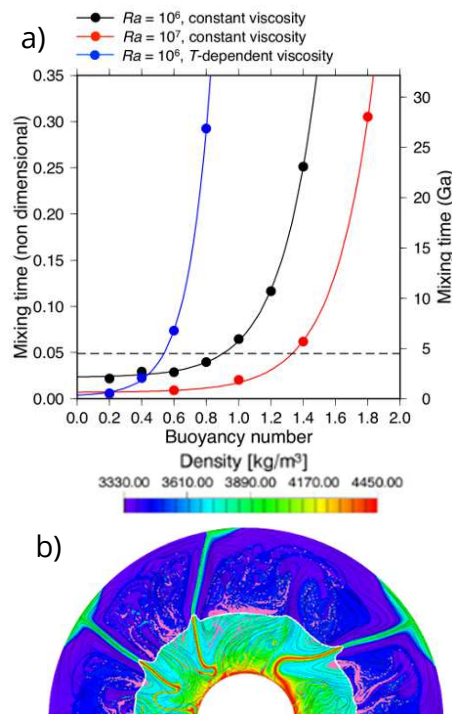


Fig. 1: a) Mixing time as a function of the buoyancy number for systems heated from below with constant (black and red lines) and temperature-dependent viscosity (blue line). The density gradient corresponding to $B = 0.2 - 2.0$ varies between $27 - 244 \text{ kg/m}^3$; b) chemical density distribution during the mantle overturn, when using the initial density profile from [5, 7].

When using the complex magma ocean initial density profile from [5, 7], where density gradient exceeds 600 kg/m^3 ($B > 3.3$), a stagnant lid forms rapidly be-

cause of the strong temperature dependence of the viscosity.

Assuming that the stagnant lid will break (Fig. 1b), a stable density gradient is obtained, due to sinking of the densest material and thus of the entire amount of heat sources, initially located close to the surface, to the core-mantle-boundary. Thermal convection is suppressed by the strong chemical gradient and the inefficient heat transport together with the concentration of heat producing elements in a thin layer located above the core-mantle-boundary lead to a strong overheating of the lowermost mantle, whose temperature increases to values that exceed the liquidus [9].

In the second scenario, density variations associated with partial melting and mantle depletion lead as well to the formation of early distinct geochemical reservoirs but also a long-lived partial melt production in the mantle. Here, we assume that early in its evolution Mars experienced a large degree of partial melting but no global magma ocean.

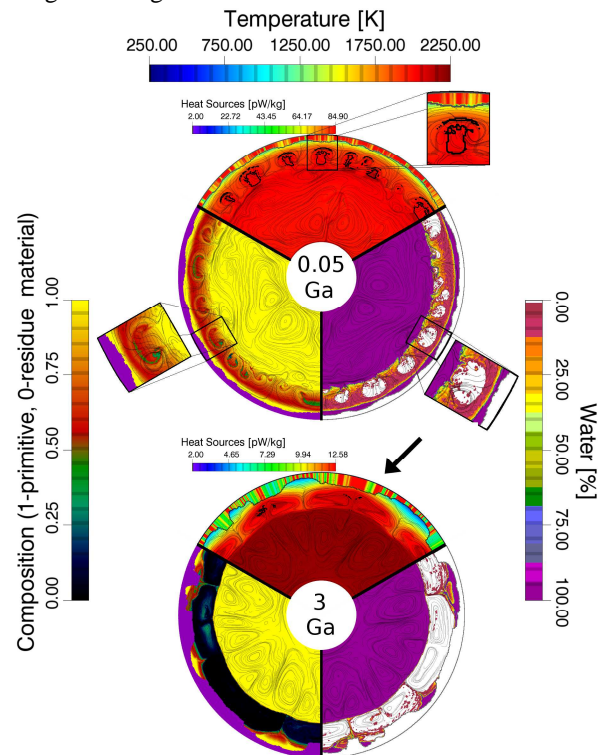


Fig. 2: Temperature, composition (mantle depletion) and water content distribution during the thermal evolution, where a density difference of 60 kg/m^3 between primitive and depleted mantle material was used. The arrow indicates the location of a stable upwelling in the upper depleted mantle, which forms around 1 Ga. Black contour lines show the partial melt regions.

The most important parameter influencing the thermo-chemical evolution is the assumed density dif-

ference between the primitive and the depleted mantle material (i.e., between peridotite and harzburgite). With small values of compositional buoyancy, crustal formation including crustal delamination is very efficient, also resulting in efficient processing and degassing of the mantle. The entire convecting mantle below the stagnant lid depletes continuously with time. In contrast, with increasing compositional buoyancy (a density gradient of up to 60 kg/m^3), crustal formation and mantle degassing are strongly suppressed although partial melting is substantially prolonged in the thermal evolution due to an insulating crust and a depleted and positively buoyant upper mantle, both of which help maintaining the underlying mantle warm (Fig. 2). The crust shows strong lateral variations in thickness, and crustal delamination is reduced and occurs only locally. Furthermore, two to four different mantle reservoirs can form depending on the initial temperature distribution [10]. Some of these reservoirs can be sustained during the entire evolution whereas others change with time.

Conclusions: To build early and stable geochemical reservoirs and to further explain the observed volcanic history of Mars [8, 9], specific requirements on compositional density variations in the mantle are necessary and limit possible evolution scenarios. Large density gradients ($> 600 \text{ kg/m}^3$), as suggested from models of the fractional crystallization of a global magma ocean, lead to the formation of distinct reservoirs but, in the absence of convective stirring inhibited by the stable configuration, these remain separated for the rest of the thermo-chemical evolution of Mars and thus ‘untraceable’. Furthermore, the magma ocean model cannot be reconciled with the expected prolonged volcanic activity.

The scenario of early partial melting and the associated density variation in the order of $20 - 60 \text{ kg/m}^3$ can better explain the reservoir formation and observed volcanic history. However, it still remains to be clarified if the isotopic signatures of the SNCs are compatible with this model.

References: [1] Foley C. N. et al. (2005) *GCA*, 69, 4557–4571. [2] Papike J. J. et al. (2009) *GCA*, 73, 7443–7485. [3] Tosi N. et al. (2010) *EPSL*, 298, 229–243. [4] Hüttig C. and Stemmer K. (2008) *PEPI*, 171, 137–146. [5] Elkins-Tanton L. T. et al. (2003) *MPS*, 38, 12, 1753–1771. [6] Debaille V. et al. (2009) *Nature Geoscience*, 2, 548–552. [7] Elkins-Tanton L. T. et al. (2005) *EPSL*, 236, 1–12. [8] Tosi N. et al. (2013) *JGR*, 118, 7, 1512–1528. [9] Plesa A. C. et al. *EPSL* submitted. [10] Plesa A. C. and Breuer D. (2013) *PSS*, in press.